Research Square

Preprints are preliminary reports that have not undergone peer review.
They should not be considered conclusive, used to inform clinical practice,
or referenced by the media as validated information.

Longitudinal Resting-State fMRI Reveals Temporal Evolution of Network-Level Alterations in a Mouse Model of Tinnitus

Tengfei Qu
Capital Medical University
Wei Zhang
zhangwei198211010163.com
China Academy of Chinese Medical Sciences
Binbin Nie
The Institute of High Energy Physics of the Chinese Academy of Sciences
Jie Wang
National Center for Magnetic Resonance in Wuhan, Chinese Academy of Sciences-Wuhan National Laboratory for Optoelectronics
Zhengde Du
Capital Medical University

Research Article

Keywords: Tinnitus, Resting-state functional magnetic resonance imaging (rs-fMRI), Functional connectivity, Fractional amplitude of low-frequency fluctuations (fALFF), Regional homogeneity (ReHo)

Posted Date: March 25th, 2026

DOI: https://doi.org/10.21203/rs.3.rs-9089544/v1

License: This work is licensed under a Creative Commons Attribution 4.0 International License.
Read Full License

Additional Declarations: No competing interests reported.

Longitudinal Resting-State fMRI Reveals Temporal Evolution of Network-Level Alterations in a Mouse Model of Tinnitus

Tengfei Qu[a#], Wei Zhang[b*], Binbin Nie[c], Jie Wang[d], Zhengde Du[a]

[a] Department of Otolaryngology Head and Neck Surgery, Beijing Friendship Hospital, Capital Medical University, 95 Yong'an Road, Xicheng District, Beijing, 100050, China.

[b] Department of Otolaryngology, Ophthalmology Hospital, China Academy of Chinese Medical Sciences, No. 33 Lugu Road, Shijingshan District, Beijing, 100040, China.

[c] The Institute of High Energy Physics of the Chinese Academy of Sciences, 19B Yuquan Rd, Shijingshan District, Beijing, 100049, China.

[d] Key Laboratory of Magnetic Resonance in Biological Systems, State Key Laboratory of Magnetic Resonance and Atomic and Molecular Physics, National Center for Magnetic Resonance in Wuhan, Wuhan Institute of Physics and Mathematics, Innovation Academy for Precision Measurement Science and Technology, Chinese Academy of Sciences-Wuhan National Laboratory for Optoelectronics, Wuhan, 430071, China..

[#]These authors contributed equally to this work.

***Corresponding Authors**:

Wei Zhang, PhD, Department of Otolaryngology, Ophthalmology Hospital, China Academy of Chinese Medical Sciences, No. 33 Lugu Road, Shijingshan District, Beijing, 100040, China, Email: zhangwei19821101@163.com.

Declarations

Ethics approval and consent to participate: All animal experiments were approved by the Animal

Care and Use Committee of Capital Medical University (Approval No. AEEI-2017-112). All methods were carried out in accordance with relevant guidelines and regulations.

Consent for publication: Not applicable.

Availability of data and material: The data that support the findings of this study are available from the corresponding author upon reasonable request.

Competing interests: The authors declare that they have no competing interests.

Funding: The work was supported by beijing natural science foundation (grant No. 7252274); and Sponsored by National Natural Science Foundation of China (grant No. 82205206).

Abstract

Tinnitus, one of the most common hearing disorders, profoundly impacts patients' quality of life, often leading to severe emotional distress and sleep disturbances. Despite its clinical burden, therapeutic options remain limited due to an incomplete understanding of its pathophysiology. While cochlear damage is a known trigger, accumulating evidence suggests that maladaptive central plasticity—particularly in non-auditory networks—plays a central role in the chronicity of tinnitus. Specifically, limbic structures (hippocampus, amygdala) and striatal regions (caudate putamen) show altered functional connectivity with auditory nuclei in both human fMRI and animal models. To systematically map these network-level changes, we employed a noise-induced tinnitus mouse model and performed longitudinal resting-state BOLD fMRI across 27 brain regions of interest (ROIs). Our multi-time point analysis revealed early phase hyperactivity (days 1 and 7 post-injury) in auditory thalamocortical pathways, consistent with compensatory gamma oscillation mechanisms. This was followed by delayed limbic-striatal engagement (day 28), characterized by enhanced hippocampal-amygdala connectivity and caudate putamen dysregulation, which aligns with human studies of tinnitus-related emotional processing. We observed a dynamic network expansion over time, where initially localized auditory abnormalities progressively recruited the default mode and salience networks. These findings validate the 'central gain reorganization' hypothesis and highlight novel therapeutic targets. Notably, the caudate putamen emerged as a key modulator in the gating of phantom sound perception, suggesting the potential efficacy of striatal-directed neuromodulation. This work bridges translational gaps by demonstrating that tinnitus is a whole-brain disorder requiring network-level interventions, paving the way for personalized neuromodulatory strategies.

Keywords: Tinnitus, Resting-state functional magnetic resonance imaging (rs-fMRI), Functional connectivity, Fractional amplitude of low-frequency fluctuations (fALFF), Regional homogeneity (ReHo)

Introduction

Tinnitus, a phantom auditory perception affecting 10–15% of the global population, is frequently accompanied by debilitating comorbidities such as insomnia, anxiety, and cognitive deficits[1-3]. Despite therapeutic advancements, over 60% of patients exhibit treatment resistance, underscoring the need to clarify the disorder's neurobiological basis[4,5]. The etiology remains debated, balancing between peripheral cochlear insults and maladaptive central nervous system (CNS) reorganization[6,7]. The historical "central gain enhancement" model posits that cochlear damage triggers compensatory hyperexcitability in central auditory circuits[8-10]. However, this fails to explain tinnitus in individuals without hearing loss[10,11]. The "prefrontal-striatal gating" model suggests that tinnitus arises from a malfunction in thalamic-limbic noise cancellation systems, implying that peripheral damage alone is insufficient[12]. Consequently, research has shifted toward large-scale brain networks. The default mode network (DMN), attention networks, and limbic structures are implicated, given the disorder's persistence during quiet states and its frequent association with emotional distress[13,14]. Resting-state fMRI (rs-fMRI) evidence reveals altered functional connectivity (FC) between auditory and limbic regions, such as the amygdala and thalamus, indicating a distributed network pathology[15].

Critical gaps remain, as most studies are cross-sectional and fail to capture the temporal dynamics of network dysfunction or the interaction between peripheral degeneration and central pathologies. To address these limitations, we developed a validated chronic tinnitus mouse model and employed longitudinal resting-state BOLD fMRI to map whole-brain activity across 27 regions. Our findings reveal a paradox: increased activity in the auditory cortex and limbic structures coexists with reduced FC between auditory pathways and limbic nodes. These alterations correlate with behavioral distress, suggesting a network-level disruption in emotional-auditory integration. By integrating longitudinal neuroimaging with computational modeling, this study redefines tinnitus as a disorder of dynamic network equilibrium.

Materials and Methods

Study Design and Animals

Male C57BL/6J mice (5 weeks old, normal hearing) were housed in a low-noise environment with a reversed 12/12 h light/dark cycle at constant temperature (20–22°C) and humidity (60–70%). After one week of acclimatization, mice (n = 12) were exposed binaurally to 100 dB SPL white noise for 2 hours. Sex- and age-matched unexposed mice (n = 10) served as controls. Auditory brainstem response (ABR), acoustic startle reflex (ASR), and gap prepulse inhibition of the acoustic startle reflex (GPIAS) were measured on days 1, 7, and 28 post-exposure. Functional neural activity and connectivity were assessed using resting-state BOLD fMRI at the same time points.(Figure 1) All animal experiments were approved by the Institutional Animal Care and Use Committee of Capital Medical University (AEEI-2017-112).

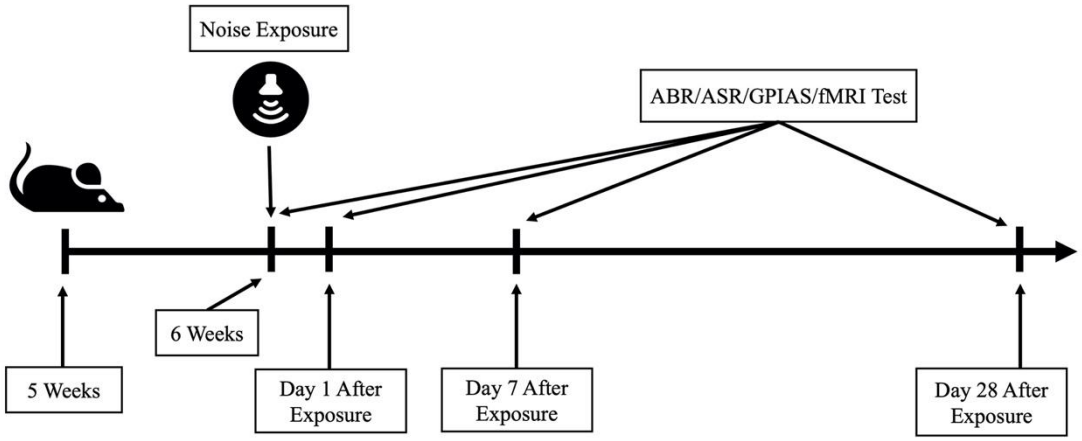


Figure 1. Timeline of the experimental procedures. ABR, auditory brainstem response; ASR, acoustic startle reflex; GPIAS, gap-prepulse inhibition of the acoustic startle reflex; fMRI, functional magnetic resonance imaging.

Noise Exposure

White noise was synthesized using Cool Edit Pro (Adobe Systems), amplified by a Crown XTi 4002 amplifier, and played through two JBL KP6000 loudspeakers mounted on either side of the mouse cages. Experimental mice were exposed to 100 dB SPL white noise in both ears for 2 h in a soundproof room while awake and unrestrained in subdivided stainless steel wire cages placed directly between the loudspeakers. Noise calibration to the target SPL was performed before each exposure session.

Auditory Brainstem Response (ABR) Recording

After anesthesia (ketamine, 100 mg/kg; xylazine, 10 mg/kg, i.p.), mice were placed on a heating pad in an audiometric chamber. Subdermal needle electrodes were placed at the vertex (+), below the pinna of the test ear (-), and in the contralateral ear (ground). Tone bursts (5 ms duration) at 4, 8, 16, and 32 kHz were generated using Tucker-Davis Technologies (TDT) hardware. ABR waves were recorded with an average of 1024 responses at 5-dB intervals. The lowest stimulus level at which ABR waves could be reliably detected was defined as the threshold.

Acoustic Startle Reflex (ASR)

Mice were placed in a wire mesh cage on a sensitive piezoelectric transducer platform inside a soundproof, dark chamber. Narrow-band noise bursts (20 ms, centered at 4, 8, 16, and 32 kHz, 60–100 dB SPL) were used as startle stimuli. The amplitude of the startle response was recorded as the maximum pressure within 250 ms after stimulus onset. The inter-trial interval was randomly varied between 16 s and 24 s.

Gap-Prepulse Inhibition of the Acoustic Startle Reflex (GPIAS)

During GPIAS testing, continuous background carrier tones (4, 8, 16, and 32 kHz at 70 dB SPL) were maintained. For gap trials, a silent gap (75 ms) was embedded in the tone 100 ms before the startle pulse (120 dB SPL broadband noise, 20 ms). Testing included “gap” and “no-gap” trials. The inhibition ratio was calculated as 1 minus (gap response amplitude / no-gap response amplitude). A reduced inhibition ratio indicated impaired gap detection, a behavioral hallmark of tinnitus.

MRI Data Acquisition

For MRI studies, mice were initially anesthetized with 3.0–4.0% isoflurane (1:4 O2/air mixture). To

minimize the influence of anesthesia on BOLD signals, medetomidine (0.3 mg/kg, i.p.) was administered, and the gas mixture was switched to normal air. Mice were placed prone in the scanner with the head stabilized using a bite bar and ear bars. Physiological parameters (respiration rate, oxygen saturation, and temperature) were monitored and maintained within normal ranges.

Imaging was performed on a 7.0-T PharmaScan MRI scanner (Bruker Biospin). A volume coil was used for transmission, and a custom-designed surface coil for reception. Functional imaging was acquired using gradient-echo echo-planar imaging (GE-EPI) with TR = 2000 ms, TE = 15 ms, matrix size = 64 × 64, FOV = 20 × 20 mm^2, and 15 axial slices. Resting-state fMRI was acquired for 10 min (300 volumes). High-resolution T2-weighted anatomical images were acquired for registration.

MRI Data Processing and Statistical Analysis

All functional image post-processing was performed by an observer blinded to group identity using SPM8 and DPARSF software. Preprocessing steps included: discarding the first 10 volumes, slice timing correction, realignment, spatial normalization to a mouse brain template (Paxinos & Franklin space), smoothing (2 × 2 × 2 mm^3 FWHM), and linear trend removal.

Amplitude of Low-Frequency Fluctuations (ALFF) and fractional ALFF (fALFF) were calculated to quantify spontaneous neural activity. Regional Homogeneity (ReHo) was computed to assess local synchronization of neural activity. For functional connectivity (FC) analysis, the brain was segmented into 27 regions of interest (ROIs) based on a mouse brain atlas. Time courses were extracted from each ROI, and Pearson correlation coefficients were calculated between all ROI pairs to construct whole-brain FC maps.

Statistical Analysis

Statistical analyses were performed using GraphPad Prism 7 and SPSS 13.0. Normality was assessed using the Kolmogorov–Smirnov test, and homogeneity of variance was assessed using Bartlett's test. Group differences in ABR thresholds, ASR, and GPIAS were analyzed using two-way ANOVA followed by Bonferroni post-hoc tests. Differences in fMRI metrics (fALFF, ReHo, FC) between experimental and control groups were analyzed using independent-samples t-tests. A p-value < 0.05 was considered statistically significant. For voxel-wise analyses, a cluster-level False Discovery Rate (FDR) correction was applied.

Results

3.1 Spatiotemporal Dynamics of Functional Connectivity

To investigate the spatiotemporal alterations in functional connectivity (FC) associated with tinnitus, we performed longitudinal comparisons between tinnitus and control mice at three time points: 1, 7, and 28 days post-exposure. Our analysis revealed a progressive reorganization of brain networks, evolving from localized auditory deficits to widespread network dysfunction.

During the acute phase (Day 1), the overall FC strength between most brain regions remained comparable to that of controls. However, specific localized alterations were evident. We observed a significant decrease in FC between the inferior colliculus (IC) and cochlear nucleus (CN), as well as between the auditory cortex (ACx) and hippocampus (HIP). Conversely, connectivity between the magnocellular nucleus of the lateral hypothalamus (MCLH) and somatosensory cortex (SSCx) was significantly increased (Figure 2; $p < 0.05$).

As the condition progressed, the network reorganization extended beyond primary auditory nuclei. By Day 7 (subacute phase), the number of brain regions exhibiting significant FC changes increased,

indicating a progressive recruitment of adjacent auditory-related areas. By Day 28 (chronic phase), widespread network alterations were observed. Both the number of significantly altered FC links and their magnitude were markedly elevated relative to controls. Specifically, the medial geniculate body (MGB), auditory cortex, hippocampus, and hypothalamic regions showed the most significant decrements in connectivity. Furthermore, the caudate putamen (CPu) exhibited altered connectivity with the SSCx and other regions.

Notably, the quantitative trajectory of these connectivity changes is illustrated in Figure 3, which details the variations in FC between specific ROIs across all three time points. This visualization underscores the transition from early auditory decoupling to later limbic-striatal dysregulation. As summarized in Table 1, the number of regions of interest (ROIs) displaying significant FC changes increased over the 28-day period, confirming the shift from localized auditory abnormalities to distributed network dysfunction..

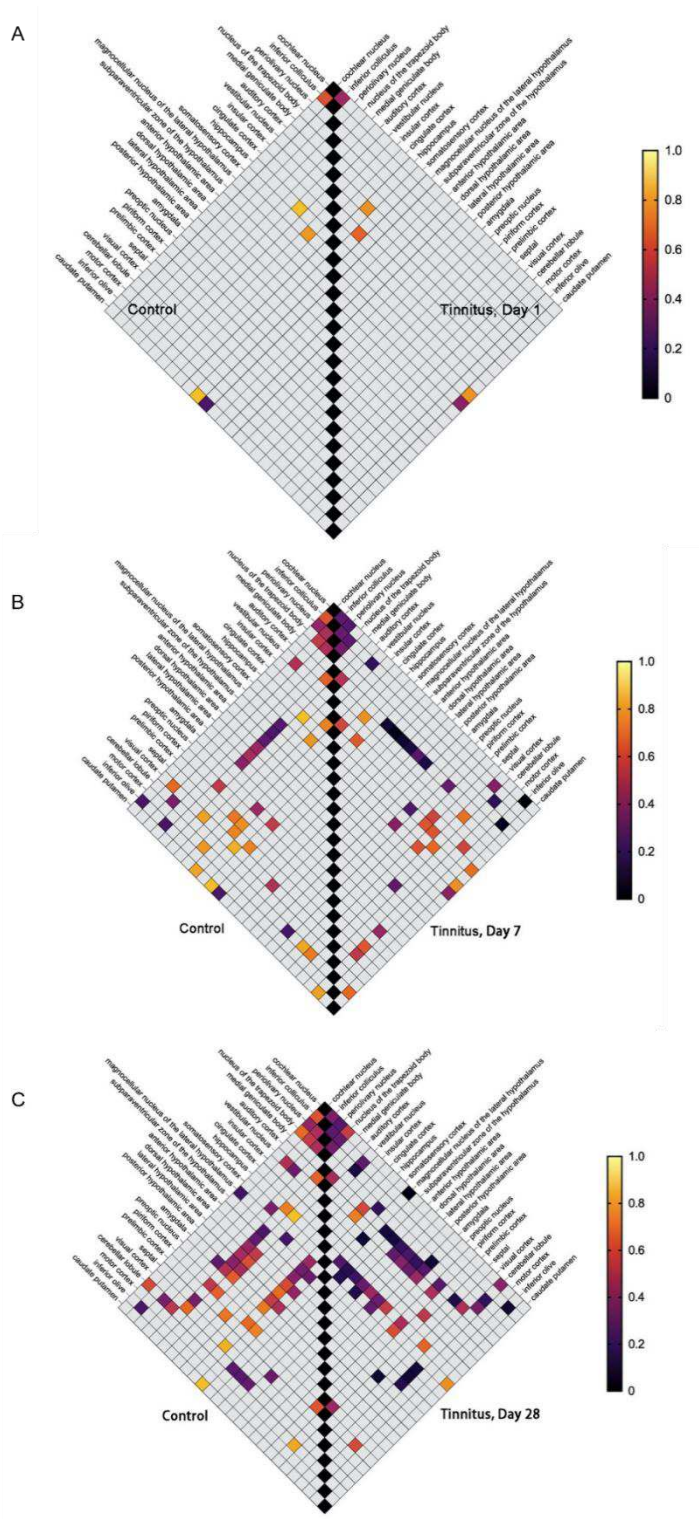


Figure 2. Variations in functional connectivity between pairwise brain regions at day 1 in tinnitus mice compared to controls. The diagram on the left shows regions of interest with significant changes: ACx-HIP (A), IC-CN (B), SSCx-ICx ©, CPu-SSCx (D), MCLH-SSCx (E). The right histogram displays significantly decreased functional correlation (A'-D') and increased correlation (E'). Data are mean ± SD; $p < 0.05$.

Table 1. Statistical results of the number of brain regions of interest showing significant changes in functional connectivity at day 1, 7, and 28 in tinnitus mice (n = 12)

Brain Regions of Interest	Day 1	Day 7	Day 28
cochlear nucleus	1	3	5
inferior colliculus	1	5	5
periolivary nucleus	——	4	5
nucleus of the trapezoid body	——	3	6
medial geniculate body	——	8	11
auditory cortex	1	2	7
vestibular nucleus	——	1	3
insular cortex	1	4	1
cingulate cortex	——	5	——
hippocampus	1	1	11
somatosensory cortex	2	4	6
magnocellular nucleus of the lateral hypothalamus	1	1	4
subparaventricular zone of the hypothalamus	——	1	4
anterior hypothalamic area	——	1	3
dorsal hypothalamic area	——	2	5
lateral hypothalamic area	——	1	3
posterior hypothalamic area	——	1	4
amygdala	——	——	4
caudate putamen	2	3	1
piriform cortex	——	1	5
prelimbic cortex	——	3	3
septal	——	3	2
visual cortex	——	4	2
cerebellar lobule	——	1	6
motor cortex	——	5	1
inferior olive	——	2	1
preoptic nucleus	——	3	——

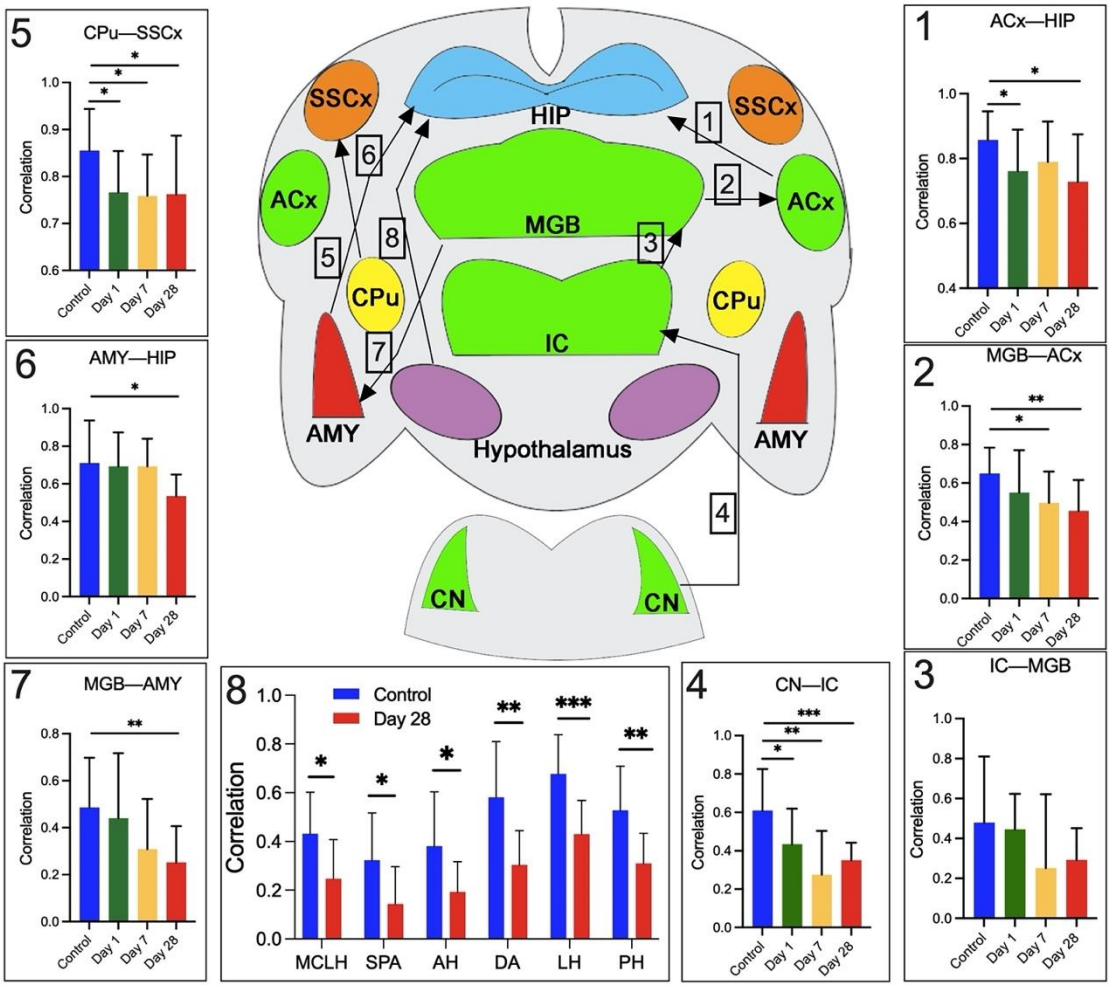


Figure 3. The histogram showed variations in functional connectivity between the certain brain regions of interest at day1, 7 and 28 in tinnitus mice after noise exposure (n = 12), as compared with control.

Mean ± SD, statistical significance by independent-samples t-tests as compared with baseline/control: $p < 0.05$, $p < 0.01$, $p < 0.001$.

3.2 Spontaneous Neural Activity Measured by fALFF

We evaluated spontaneous neural activity using the fractional amplitude of low-frequency fluctuations (fALFF) to assess local metabolic intensity. In the acute phase (Day 1), significant increases in fALFF were observed in the amygdala, auditory cortex, caudate putamen, hippocampus, and insular cortex ($p < 0.005$), indicating widespread hyperactivity.

By Day 7, this hyperactivity persisted in the amygdala and caudate putamen, whereas activity levels decreased in some auditory regions. At the chronic phase (Day 28), elevated fALFF remained prominent in the amygdala, hippocampus, and olfactory regions, suggesting sustained hyperactivity in limbic and associated areas (Figure 4).

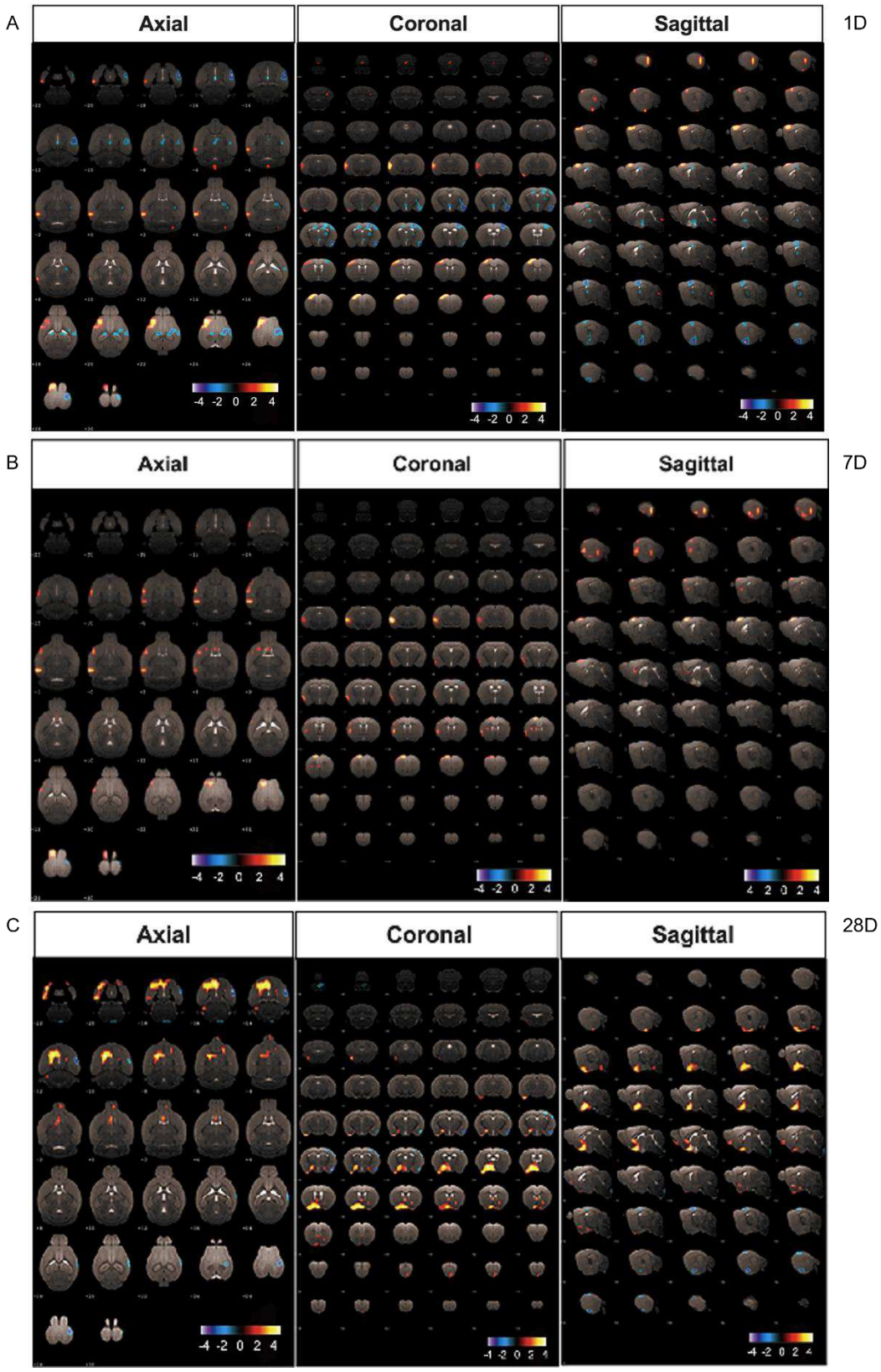


Figure 4. Functional connectivity heatmaps and fALFF analysis maps illustrating the progressive enhancement of connectivity and local synchronization deficits over the 28-day period.

3.3 Local Neural Synchronization Measured by ReHo

Regional Homogeneity (ReHo) analysis was conducted to assess the local synchronization of neural activity. The results indicated time-dependent deficits in local coordination. On Day 7, significant increases in ReHo were noted in the amygdala, caudate putamen, and hippocampus, reflecting enhanced local synchronization within these limbic-striatal circuits.

By Day 28, these alterations had extended to the substantia nigra and visual cortex, indicating broader network dysregulation (Figure 5). The coexistence of increased ReHo (local synchronization) with decreased long-range FC in regions like the hippocampus and amygdala suggests a decoupling of local processing from global network integration.

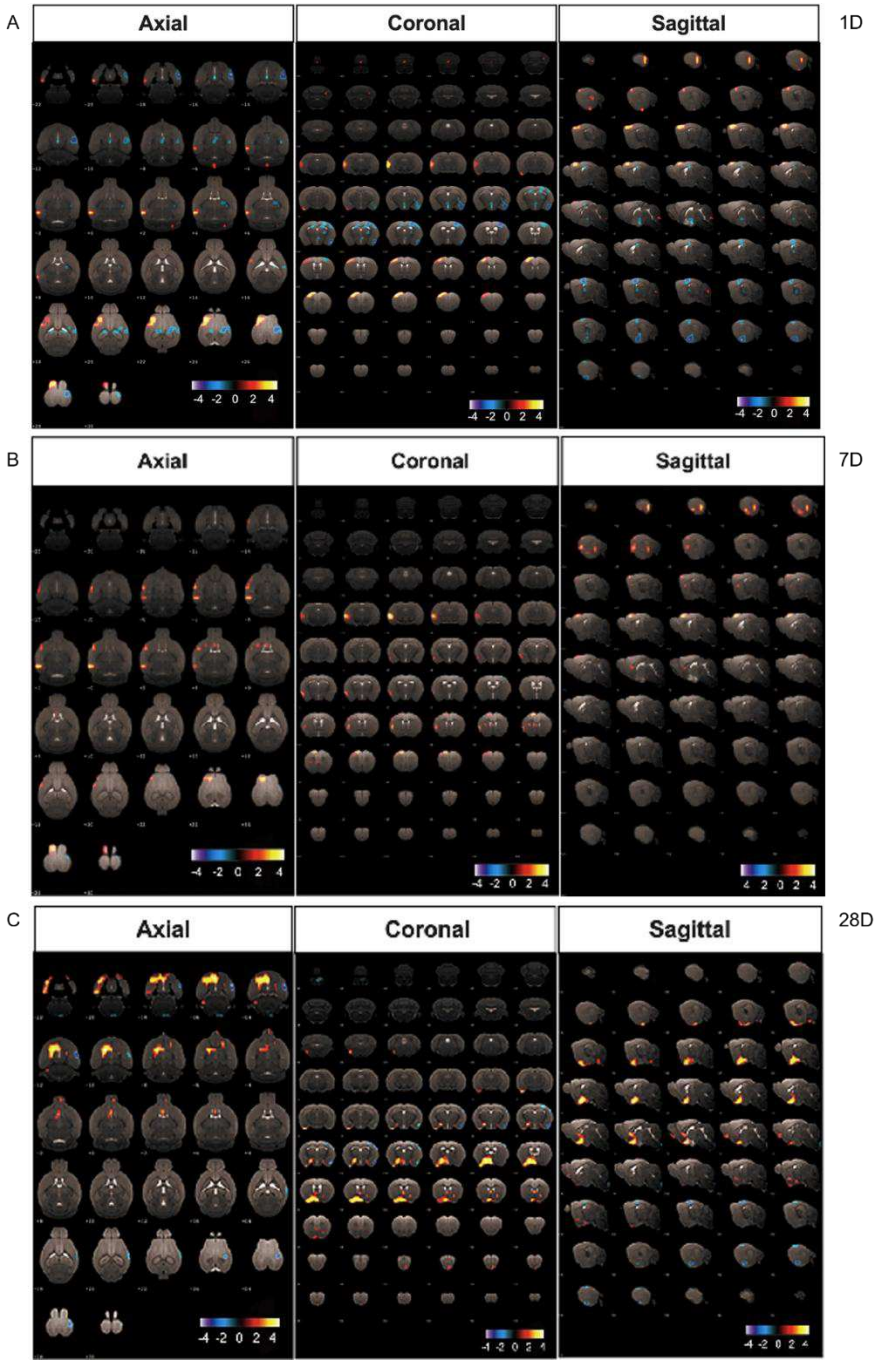


Figure 5. Functional connectivity heatmaps and ReHo analysis maps illustrating the progressive enhancement of connectivity and local synchronization deficits over the 28-day period.

Discussion

Temporal Evolution of Tinnitus Pathophysiology

Guided by established definitions of acute (≤14 days) and chronic (≥28 days) phases in rodent models, our longitudinal study delineates a clear spatiotemporal trajectory of tinnitus-related network dysfunction. The observed connectivity alterations suggest that tinnitus initiation predominantly engages auditory system plasticity, while chronicization involves large-scale network shifts where limbic structures (amygdala, hippocampus) and affective circuits assume greater functional significance. This reinforces the concept that tinnitus is not merely an auditory disorder but a systemic condition involving emotional, cognitive, and autonomic networks.

The Role of Auditory Pathways: Acute and Subacute Phases

In the acute phase (Day 1), our study demonstrated significant reductions in functional connectivity (FC) within hierarchical auditory pathways, specifically between the Cochlear Nucleus (CN), Inferior Colliculus (IC), Medial Geniculate Body (MGB), and Auditory Cortex (ACx). These FC declines reflect disrupted neuronal synchrony within the ascending auditory system following noise trauma.

Mechanistically, this desynchronization is likely driven by an excitation-inhibition (E/I) imbalance. Noise trauma depletes GABAergic interneurons in the CN and IC, reducing inhibitory tone while enhancing glutamatergic drive. This amplification of neural noise disrupts thalamocortical rhythms, specifically leading to aberrant gamma oscillations in the ACx. Furthermore, microglial activation and synaptic pruning in the IC and MGB may contribute to the breakdown of frequency-specific information transfer. Our finding that the summed FC reduction across CN-IC-MGB-ACx nodes strongly correlates with tinnitus severity in gap detection tests supports the critical role of early auditory decoupling in tinnitus perception.

Mechanisms of Chronic Tinnitus: Limbic and Striatal Engagement

By Day 28, our analysis revealed extensive FC reductions in non-auditory regions, particularly the hippocampus, amygdala, and hypothalamus. This network decentralization highlights their pivotal roles in tinnitus chronicization.

MGB-Amygdala Circuit: The reduction in FC between the MGB and amygdala reflects disrupted emotional salience encoding. GABAergic disinhibition in the amygdala prevents the proper gating of phantom sounds, leading to increased anxiety and aversive responses to tinnitus.

ACx-Hippocampus Circuit: Reduced FC between the ACx and hippocampus suggests defective theta-gamma coupling, which is critical for memory consolidation. This may explain the persistence of the tinnitus percept as a maladaptive "engram" that is resistant to extinction.

Somatosensory Cortex-Caudate Putamen (CPu): The CPu acts as a sensorimotor gate. Reduced FC between the somatosensory cortex and CPu, coupled with dopaminergic dysregulation, impairs the filtering of somatic inputs (e.g., jaw or neck movements), allowing irrelevant signals to modulate the tinnitus percept.

Hippocampus-Hypothalamus Circuit: The disruption of this circuit mediates autonomic and sleep disturbances associated with tinnitus. FC decline correlates with sympathetic overdrive and sleep fragmentation, common comorbidities in chronic tinnitus patients.

Therapeutic Implications

Our findings suggest that effective treatment for chronic tinnitus must target the broader network rather than the auditory cortex alone.

Neuromodulation: Closed-loop deep brain stimulation (DBS) targeting the hippocampus-amygdala

theta coherence could normalize emotional processing. Additionally, bimodal neuromodulation (e.g., vagus nerve stimulation paired with sound) shows promise in restoring auditory-limbic connectivity.
Pharmacotherapy: Agents targeting neuroplasticity, such as BDNF/TrkB agonists for the hippocampus or CRF1 receptor antagonists for the amygdala, may reverse the maladaptive network reorganization.
Precision Medicine: Stratifying patients based on connectome profiles (e.g., those with dominant limbic vs. striatal dysfunction) could improve the efficacy of interventions like repetitive transcranial magnetic stimulation (rTMS).

Conclusion and Future Perspectives

Our longitudinal fMRI study demonstrates that tinnitus is a disorder of dynamic network equilibrium, evolving from localized auditory hyperactivity to widespread limbic-striatal dysregulation. The identification of specific network bottlenecks—such as the caudate putamen and hippocampal-amygdala circuitry—provides novel targets for neuromodulation. Future research should focus on translating these preclinical findings into clinical trials using biomarker-driven stratification, ultimately moving from symptom management to disease-modifying therapies.

Reference

1. Langguth, B., and De Ridder, D. (2024). Tinnitus, Tinnitus Disorder, and Other Phantom Perceptions. In Textbook of Tinnitus, (Springer), pp. 17-24.
2. Langguth, B., De Ridder, D., Schlee, W., and Kleinjung, T. (2024). Tinnitus: clinical insights in its pathophysiology-a perspective. Journal of the Association for Research in Otolaryngology *25*, 249-258.
3. Henry, J.A., Reavis, K.M., Griest, S.E., Thielman, E.J., Theodoroff, S.M., Grush, L.D., and Carlson, K.F. (2020). Tinnitus: an epidemiologic perspective. Otolaryngologic Clinics of North America *53*, 481-499.
4. Pineault, D. (2024). From Tinnitus to Musical Hallucinations: Navigating Complex Auditory Symptoms. Canadian Audiologist *11*.
5. Baguley, D., McFerran, D., and Hall, D. (2013). Tinnitus. The Lancet *382*, 1600-1607.
6. Baguley, D.M. (2002). Mechanisms of tinnitus. British medical bulletin *63*, 195-212.
7. Langguth, B., Elgoyhen, A.B., and Cederroth, C.R. (2019). Therapeutic approaches to the treatment of tinnitus. Annual review of pharmacology and toxicology *59*, 291-313.
8. Auerbach, B.D., Rodrigues, P.V., and Salvi, R.J. (2014). Central gain control in tinnitus and hyperacusis. Frontiers in neurology *5*, 206.
9. Hayes, S.H., Schormans, A.L., Sigel, G., Beh, K., Herrmann, B., and Allman, B.L. (2021). Uncovering the contribution of enhanced central gain and altered cortical oscillations to tinnitus generation. Progress in Neurobiology *196*, 101893.
10. Parameshwarappa, V., and Norena, A.J. (2024). Central Gain Model for Tinnitus: A Review on Noise-Induced Plasticity or When Less at the Periphery Is More in the Center. Textbook of Tinnitus, 205-219.
11. Waechter, S., and Jönsson, A. (2022). Hearing aids mitigate tinnitus, but does it matter if the patient receives amplification in accordance with their hearing impairment or not? A meta-analysis. American Journal of Audiology *31*, 789-818.
12. Kollias, P. (2022). Corticostriatal Mechanisms of Gating Working and Short-Term Memories. (Princeton University).

13. Xie, J., Zhang, W., Yu, C., Wei, W., Bai, Y., Shen, Y., Yue, X., Wang, X., Zhang, X., and Shen, G. (2024). Abnormal static and dynamic brain network connectivity associated with chronic tinnitus. Neuroscience *554*, 26-33.
14. Lan, L., Liu, Y., Wu, Y., Xu, Z.-G., Xu, J.-J., Song, J.-J., Salvi, R., Yin, X., Chen, Y.-C., and Cai, Y. (2022). Specific brain network predictors of interventions with different mechanisms for tinnitus patients. EBioMedicine *76*.
15. Du, H., Feng, X., Qian, X., Zhang, J., Liu, B., Huang, Z., and Gao, X. (2022). Hearing loss and tinnitus: Uncover the mechanism of tinnitus using resting-state functional magnetic resonance imaging (rs-fMRI) technologies. medRxiv, 2022.2006. 2026.22276920.